Brownian Motion From Internal Friction

Gabriela I. González and Peter R. Saulson

Department of Physics, Syracuse University

Syracuse, NY USA 13244-1130

Abstract

We constructed a torsion pendulum in which the dissipation is dominated by internal friction in the nylon suspension fiber. We compare the measured thermal noise power spectrum with the spectrum predicted from the measured admittance via the fluctuation-dissipation theorem. The agreement between the two is excellent. The spectrum exhibits an approximately 1/f slope below resonance. We discuss the implications for interferometric detectors of gravitational waves.

Keywords: Brownian motion, thermal noise, fluctuation-dissipation theorem, gravitational wave detection.

1. Introduction

In many precision experiments, Brownian motion (also known as thermal noise) is a fundamental limit to the instrument's sensitivity. This was recognized early in the century[1]. The torsion pendulum was a favorite object of study, since it was the main element in galvanometers, radiometers and electrometers, among other sensitive instruments. Brownian motion amplitudes were measured with exquisite precision for a suspended mirror at different pressures [2] and in a galvanometer with different electromagnetic damping conditions [3]. While it was noted that the character of the pendulum motion depended on the dissipation, it was proved that in all cases the r.m.s. amplitude was independent of it; the latter's value is determined by the equipartition theorem.

When a measurement involves signals in a broad range of frequencies, the calculation of the limiting thermal noise has to be done using the fluctuation-dissipation theorem[4]. The theorem predicts the power spectrum of thermal noise, when the dissipative part of the admittance is known. In some systems, like torsion balances in experiments to test the Principle of Equivalence [5], as well as in the test masses of interferometric gravitational wave detectors [6, 7, 8], the energy dissipation will usually be due to internal friction in the wires and/or

masses of the pendulums. As a function of frequency, dissipation due to internal friction may have a very different behavior from the best known example for energy loss, viscous friction. The implications are dramatic: below a resonance, the thermal noise spectrum has a $1/f$ law if the dissipation is due to frequency independent internal friction, as opposed to a constant level if the dissipation is viscous [10]. For a given Q at resonance, this may change the thermal noise limit prediction by an order of magnitude (in amplitude) at the signal frequencies.

It is important, then, to have an experiment that shows the Brownian motion spectrum when the theorem is applied to a system in which the dissipation is dominated by internal friction. We built such a system with a torsion pendulum, choosing materials and dimensions such that the internal friction is enhanced to a point that it is possible to measure the pendulum's Brownian motion in a table top experiment. In this paper, we present the experimental results, showing a comparison of the direct measurement of the Brownian motion spectrum with the prediction obtained by applying the fluctuation-dissipation theorem to the measured admittance.

The paper is organized as follows: in Section 2, we review the fluctuation dissipation theorem and its assumptions; in Section 3, we describe the experimental

set up; in Section 4, we present the experimental results; and in Section 5 we summarize and present conclusions and comments.

2. The Fluctuation-Dissipation Theorem

We follow Callen and Greene's formulation of the fluctuation-dissipation theorem [4]. They obtained a relation between the macroscopic, irreversible response of a driven dissipative system and the spontaneous fluctuations of the extensive variable of the system in equilibrium (Brownian motion). For a torsion pendulum, the extensive variable is the angle θ of the pendulum about the vertical axis. The theorem states that the power spectrum $S_\theta(f)$ of the fluctuations is related to the real part of the admittance $Y(f)$:

$$S_\theta(f) = 4k_B T \, \frac{\mathbf{Re}[Y(f)]}{(2\pi f)^2}. \tag{2.1}$$

For a mechanical system with a spring constant, we can describe the dissipation as the imaginary part of a complex spring constant. The response of the system $\theta(f)$ to a driving torque $\tau(f)$ is then related by the equation of motion

$$\left(-J\omega^2 + \kappa(1 + i\phi)\right)\theta(f) = \tau(f), \tag{2.2}$$

where J is the moment of inertia of the torsion pendulum, $\omega = 2\pi f$, and $\phi \ll 1$ is in general a function of frequency. The admittance is then

$$Y(f) \equiv \frac{i\omega\theta(f)}{\tau(f)} = \frac{i\omega}{-J\omega^2 + \kappa(1 + i\phi)}, \tag{2.3}$$

and, taking its real part, the power spectral density of the Brownian motion is

$$S_\theta(f) = \frac{4k_B T}{J\omega_0^2} \frac{\phi(f)}{2\pi f} \frac{1}{(1 - (f/f_0)^2)^2 + \phi^2(f)}, \tag{2.4}$$

with $\omega_0^2 = (2\pi f_0)^2 = \kappa/J$ being the natural frequency of the torsion pendulum.

Notice that if the dissipation mechanism is due to viscous friction (force proprtional to velocity), the loss function $\phi(f)$ is linear in frequency (if $F = -\gamma\dot{\theta}$, then $\phi(f) = 2\pi\gamma f/\kappa$). This was the case in the early experiments [2, 3], where the dissipation was due to air friction and electromagnetic damping. However, if the energy dissipation is due to internal friction, $\phi(f)$ may have a very different behavior. For most materials, it will have "Debye peaks" at certain material-dependent frequencies where a relaxation mechanism becomes important. The peaks' frequencies may be decades apart in general, and in between the peaks the function $\phi(f)$ is often approximately independent of frequency[9].

Thus, if we measure the loss function $\phi(f)$, the moment of inertia J and the resonance frequency f_0, we can use the theorem to predict the thermal noise power spectrum. The loss function can be measured by driving the system with a torque τ, measuring the pendulum frequency response

$$\chi(f) \equiv \theta(f)/\tau(f) = \left(-J\omega^2 + \kappa(1+i\phi)\right)^{-1}, \tag{2.5}$$

and then calculating the loss function as

$$\phi(f) = -\mathrm{Im}(\chi(f))/\mathrm{Re}(\chi(f)) \times (1-(f/f_0)^2). \tag{2.6}$$

On the other hand, the Brownian motion can be directly measured, and its power spectrum $S_\theta(f)$ can then be compared with the prediction based on the measurement of $\phi(f)$.

3. Experimental Apparatus

3.1. Torsion pendulum

We use a torsion pendulum as our mechanical system (Fig. 1). The pendulum mass is a rectangular Al mass, 1x1x2.5 cm, with a 4.94x0.48x0.70 cm Al piece

glued at the bottom, acting as the inertia arm. A circular mirror is glued to the front of the pendulum mass. The total pendulum mass is 10.7 gm, and its moment of inertia with respect to the vertical axis through the center of masss is J =9.92 gm-cm^2. The suspension fiber is a polyamide nylon 6 fiber from Goodfellow Inc., with a diameter of 150μm, and a length of 9.84 cm. The quoted tensile modulus is E=2.6-3.0 GPa[11]. The measured torsional frequency is f_0 =125 mHz. If we calculate the shear modulus G from the measured quantities, we obtain G = 1.2 GPa, which is consistent with a Poisson ratio v = .3 and a tensile modulus of 3.1 GPa ($G = E/(2(1+v))$).

3.2. Optical lever

To measure the angular motion of the pendulum, we used an optical lever (Fig. 2), with the beam of a 7 mW He-Ne laser being reflected from the mirror glued to the pendulum, and falling on the center of a vertically split photocell. We then measure the difference between the currents produced in each half of the photocell, since this quantity is proportional to the angle through which the mirror rotates. The lever arm from the pendulum to the photocell is D=155 cm, folded by 8 mirrors into a 30-cm diameter vacuum chamber. The laser and the photocell were

outside the vacuum chamber, but all the optical path except the first and last few mm was in vacuum. Vacuum was used for two reasons: firstly, the fiber properties were more stable than in air, where they varied with humidity; and secondly, the laser beam was more stable, avoiding variations in direction due to air density gradients. However, a rough vacuum was sufficient: measurements were done with $P \sim 1 - 50$ mtorr.

The signal was transformed into a voltage and recorded with a HP-3562A Dynamic Signal Analyzer. The system sensitivity was calibrated by putting the photocell onto a micrometer base and, with the pendulum fixed, measuring the variation of voltage with the photocell position, and then dividing this by D. With a photocurrent of about $i = 0.2$mA on each half of the photocell, the sensitivity of the optical lever was $k = 0.2$ rad/A.

3.3. Noise sources

The theoretical limiting noise in the optical lever is the shot noise in the photocurrent: this would be a white noise of amplitude $S_\theta(f) = 4eik^2 = (2 \times 10^{-12}\text{rad}/\sqrt{\text{Hz}})^2$. However, several other noise sources dominate the actual measurement, making shot noise negligible. The limiting noise in the measuring sys-

tem was measured by recording the signal with the pendulum resting on a fixed base. The main contribution to the system noise comes from laser direction stability, or beam "jitter". This jitter was proved to be lateral (as opposed to angular) noise, so we made the optical lever arm as long as possible to limit its influence in terms of angular noise.

Other modes of the system (swinging and rocking pendulum modes) are observed through misalignments: these other modes should produce a vertical displacement of the laser spot on the photocell (which ideally should not produce any signal), while the torsional mode produces a side to side displacement. However, the other pendulum modes are always strongly excited by seismic noise, and therefore they do appear in the spectrum. The pendulum is designed such that their frequencies appear at least a decade away from the torsional frequency (the pendulum frequency is 1.5 Hz, and the rocking modes are at 6 Hz and 8 Hz).

To estimate the extraneous noise other than Brownian motion affecting the measurement, we constructed two kinds of monitor signals. We split the laser beam before it hit the pendulum mirror, sending the light we picked off to another split photocell; this signal measured the laser noise, due to lateral and angular displacements, as well as intensity fluctuations. The signals from the main photo-

cell and this monitor photocell were measured simultaneously, and the coherence between these signals measured the ratio of signal to laser noise as a function of frequency. The noise measured in the monitor photocell was equivalent to a flat spectrum $S_\theta(f) = (1.4 \times 10^{-9}\text{rad}/\sqrt{\text{Hz}})^2$ between 0.3 and 10 Hz, rising with a $1/f$ power law below 0.3 Hz. The signal in the monitor photocell did not have any significant coherence with the signal in the main photocell, showing that the laser noise was not a significant fraction of the signal observed.

We monitored another sort of noise by using a quadrant photocell instead of a dual one at the output of the optical lever, allowing us to measure simultaneously the vertical and horizontal displacement of the laser spot. If the photocell is perfectly aligned with the presumably orthogonal directions of the pendulum/rocking and torsional modes, then these measurements should only show correlations for spot oscillations in some particular oblique direction (as happens when the laser is warming up, for example) or for laser intensity fluctuations. However, all modes can be observed in both signals, their ratio measuring the photocell misalignment with the modes. Even if the photocell is aligned with the vertical, it could happen that due to asymmetries in the pendulum mass, the normal modes are not aligned with gravity. In either case (principal axes or photocell misalignment), the corre-

lation of the vertical spot displacement signal with the horizontal signal measures the coupling of non-Brownian noise into the horizontal signal. If the coherence is sufficiently high, it allows for a subtraction of the noise from the signal, but even if not, it allows an estimate of the non-Brownian noise affecting the measurement.

3.4. Frequency response measurement

In order to excite the pendulum and measure its frequency response, we put two thin Al plates on opposite sides of the pendulum, facing the inertia arm (Fig. 1). A constant DC voltage $V_0 \sim 50$V plus a small AC voltage $V_{in}(t)$ was then applied to the plates, which acted as capacitors with the inertia arm, and then produced a torque whose variation was linear in $V_{in}(t)$. (The total torque is proportional to $(V_0 + V_{in}(t))^2$.) We then measure the response of the pendulum to the applied voltage $V_{in}(t)$. Notice that in order to measure the loss function $\phi(f)$ using the formula 2.6, we don't need the calibration constants of angle and torque with voltage, since we only have to measure the phase angle of the response, which is equal to the phase of $V_{out}(f)/V_{in}(f)$. This is very convenient because the torque vs. voltage constant depends on the distance between the inertia arm and the plates, which in turn depends on the equilibrium position, making it difficult to

measure precisely.

4. Experimental Results

4.1. Frequency response

We first measure the frequency response of the pendulum to the voltage applied to the capacitor plates (Fig. 3). The amplitude of the frequency response (Fig. 3a) shows the shape corresponding to 2.5, from which we can measure $f_0 = (125.5 \pm .5)$ mHz, while from the phase angle of the frequency response we can calculate the loss function using 2.6 (Fig. 3b). The function $\phi(f)$ shows a clear negative slope, which might be due to the presence of an amorphous glass transition ("α relaxation"), whose Debye peak is at a few mHz or lower at room temperature. (This is highly dependent on sample crystallinity and humidity.) Our measured $\phi(f)$ is consistent with the published data for polyamide Nylon 6 [12]. For convenience, we can represent the measured loss function with a linear relation $\phi(f)$ vs. $\log(f)$:

$$\phi(f) = (-2.8 \log(f/1\text{Hz}) + 4.7) \times 10^{-3},\ 2\text{mHz} < f < 400\text{mHz} \qquad (4.1)$$

(Note that this is an approximation valid only for the frequency range measured.) We then have all necessary "macroscopic" measurements to use the fluctuation-dissipation theorem and predict the Brownian motion spectrum, given by eqn. 2.4 (Fig. 4).

4.2. Thermal noise power spectrum

The actual measurement of Brownian motion was carried out by recording the time series $\theta(t)$ for few hours at a time, with the pendulum undisturbed by external influences. A typical portion of a time record is shown in Fig. 5. We collected about 30 hrs worth of data, in 10 different time records. With all the data, we first make a histogram of the signal amplitude, sampled at a fixed time interval and filtered through a bandpass 1mHz-1Hz; the data shows a Gaussian histogram (Fig. 6) with a root-mean-square value (the only parameter in the Gaussian) $\sqrt{\langle\theta^2\rangle} = 7.8 \times 10^{-8}$ radians. This value is within a few percent (about the error in the calibration constant) of the value predicted by the equipartition theorem: $\langle\theta^2\rangle = k_B T/J\omega_0^2 = (8.2 \times 10^{-8}\text{rad})^2$; this confirms that we are indeed observing Brownian motion.

With the data taken, we calculate the power spectral density: we divide the

time record in smaller portions (typically 400 s long), take the power spectrum (the squared modulus of the Fourier transform) of each portion, then average them to obtain the mean power spectrum. We can thus resolve frequencies from 2.5 mHz up to 2 Hz (Fig. 7).

At frequencies below the resonance, a $1/f$ power law was the general case observed down to about 10-20 mHz, but sometimes sharper departures from the $1/f$ power law could be observed. This effect varied from day to day, making the lower frequency bins not stationary. The effect also diminished when the air conditioning in the room was turned off, so it seemed to be related to temperature fluctuations or air currents.

At frequencies above resonance, the swinging pendulum mode appeared at 1.5 Hz, and the coherence between the monitor signal measuring the vertical laser spot motion and the main signal increased: a coherence of 0.4 to 1 was consistently observed between 200 mHz and 2 Hz. When the coherence was above 0.8, we take the difference between the original signal and the appropriately scaled noise measurement, and calculate the power spectrum again. Since the signals are correlated, the resultant power spectrum is smaller in the frequency band analyzed (0.15-1Hz). The rms value in this band can be reduced by as much as 40% in

some cases. Notice however, that this procedure then adds all the uncorrelated noise in the vertical and horizontal signals, for example the laser noise and shot noise, limiting the system sensitivity.

4.3. Comparison of prediction with measured spectrum

The mean power spectrum and the prediction from the fluctuation-dissipation theorem are plotted in Fig. 8, showing excellent agreement over the decade from 20 mHz to 200 mHz. The point size in the measured power spectrum points reflect the standard statistical error in the ensemble of measurements, while the error bars in the prediction line represent the margin for a 95% confidence level for the fitted function $\phi(f)$. We also draw what would have been the prediction if we had measured the Q at resonance ($Q = 96$) and had assumed that the internal friction obeyed a viscous friction model.

Note that there are no free parameters in the comparison between the predicted and measured spectra; the two spectra are derived from completely distinct sets of measurements, and each has its own independently fixed scale.

5. Discussion

It should be no surprise, perhaps, that we found a Brownian motion spectrum that agrees with the prediction of the fluctuation-dissipation theorem; the latter has been a central part of our understanding of fluctuation phenomena for the past several decades. Still, the importance of the theorem has only recently come to be fully appreciated in the segment of the experimental physics community devoted to precision mechanical measurements and gravitational physics[13],[10]. This is especially true because internal friction phenomena display a rich repertoire of behavior, seldom well-represented by a simple model of viscous friction. It can be crucial to an experiment if the thermal noise power spectrum has a $1/f$ or steeper slope below resonance, instead of the white power spectrum that comes from viscous friction.

In principle, knowledge of the functional form of the friction law should not even be required. If we are interested in the Brownian motion noise at a given frequency f, it is only necessary to know the strength of the dissipation, $\mathrm{Re}Y(f)$, at that particular frequency. Reliance on understanding the form of $\phi(f)$ comes from the fact that our most sensitive measuring instruments have often been constructed in such a way that the dissipation at the signal frequency is difficult

to measure directly. As a proxy, it has been standard practice to measure the dissipation at the frequencies at which it is easy to do so, by measuring the quality factor Q of a resonance. This can be used to extrapolate to the required quantity if and only if we know the functional form of $\phi(f)$.

The significance of correcting the earlier, less sophisticated, estimates of Brownian motion comes from a combination of two circumstances: inappropriate use of viscous friction models, and the use of quality factors measured at resonant frequencies substantially above the signal frequencies of interest. As shown in Fig. 8, this situation yields estimates of the level of the Brownian motion spectrum that are systematically low, substantially so if the ratio between resonance frequency and signal frequency is large. Recent recognition of this situation has led to increased attention being paid to the role of Brownian motion in the noise budgets both of torsion pendulum experiments and of interferometric gravitational wave detectors.

In the latter, the noise term whose importance has grown is the Brownian motion associated with the motion of the surfaces of the test masses with respect to their centers of mass. It is for these degrees of freedom that the resonances used to estimate the dissipation are substantially higher ($\sim$ 10 kHz or above)

than the signal frequencies (10 Hz to 1 kHz), the circumstance that leads to over-optimistic predictions when viscous friction models are used inappropriately. The fused silica test masses are examples of systems in which the relevant measure of dissipation, $\mathbf{Re}Y(f)$ at the signal frequency, is difficult to determine. However, a variety of measurements support the hypothesis that the loss angle $\phi(f)$ is roughly independent of frequency over the relevant frequency band in fused silica [14],[15]. This allows better founded, if less optimistic, estimates to be made.

Strong circumstantial evidence for the picture we have been sketching, and for its relevance to gravitational wave detection, comes from recent work at the Mark II 40-meter interferometer at Caltech[16]. A previously unalterable band of the 40-meter interferometer's noise power spectrum was reduced substantially when composite test masses whose resonances had poor Q values were replaced by monolithic fused silica masses with much better quality factors. The component of the noise spectrum that was reduced had the $1/f$ functional form expected from constant loss angle ϕ. The only incomplete part of the explanation is the usual inability to measure $\phi(f)$ vs. f, or alternatively $\mathbf{Re}Y(f)$ at the frequencies of interest. Note also that the dissipation in the old composite test masses was so large that it is unlikely that it is connected with whatever dissipation mechanisms

will set the fundamental limits in gravitational wave interferometers.

A new method has been proposed that should allow the internal friction to be measured at the relevant frequency scales in fused silica test masses[17]. The technique involves time domain measurements of relaxation of masses 1-100 ms after the release of a mechanical stress. If successful, it should finally allow Brownian motion of the test mass surfaces to be predicted in the straightforward way called for by the fluctuation-dissipation theorem, as illustrated in the body of the present paper.

6. Acknowledgments

We would like to thank Riley Newman, Fred Raab, Norna Robertson and Robert Spero for useful discussions. This work was supported in part by Syracuse University and by National Science Foundation Grant PHY-9113902.

References

[1] R.B. Barnes and S. Silverman, Rev. Mod. Phys. 6 (1934) 162.

[2] E. Kappler, Ann. d. Physik 11 (1931) 233.

[3] R.V. Jones and C.W. McCombie, Phil. Trans. Roy. Soc. 244 (1952) 205.

[4] H.B. Callen and R.F. Greene, Phys. Rev. 86 (1952) 702.

[5] M. A. Beilby, N. Krishnan, and R.D. Newman, in Experimental gravitation, eds. M. Karim and A Qadir (Institute of Physics Publishing, Bristol, 1994) p. A277.

[6] A. Abramovici, W.E. Althouse, R.W.P. Drever, Y. Gürsel, S. Kawamura, F.J. Raab, D. Shoemaker, L. Sievers, R.E. Spero, K.S. Thorne, R.E. Vogt, R, Weiss, S.E. Whitcomb, and M.E. Zucker, Science 256 (1992) 325.

[7] C. Bradaschia, R. Del Fabbro, A. Di Virgilio, A. Giazotto, H. Kautzky, V. Montelatici, D. Passuello, A. Brillet, O. Cregut, P. Hello, C.N. Man, P.T. Manh, A. Marraud, D. Shoemaker, J.-Y. Vinet, F. Barone, L. Di Fiore, L. Milano, G. Russo, S. Solimeno, J.M. Aguirregabiria, H. Bel, J.-P. Duruisseau, G. Le Denmat, P. Tourrenc, M. Capozzi, M. Longo, M. Lops, I. Pinto, G. Rotoli, T. Damour, S. Bonazzola, J.A. Marck, Y. Gourghoulon, L.E. Holloway, F. Fuligni, V. Iafolla, and G. Natale, Nucl. Instr. Meth. Phys. Res. A 289 (1990) 518.

[8] K. Danzmann, J. Chen, P.G. Nelson, T.M. Niebauer, A. Rüdiger, R. Schilling, L. Schnupp, K.A. Strain, H. Walther, W. Winkler, J. Hough, A.M. Campbell, C.A. Cantley, J.E. Logan, B.J. Meers, E. Morrison, G.P. Newton, D.I. Robertson, N.A. Robertson, S. Rowan, K.D. Skeldon, P.J. Veitch, H. Ward, H. Welling, P. Aufmuth, I. Kröpke, D. Ristau, J.E. Hall, J.R.J. Bennett, I.F. Corbett, B.W.H. Edwards, R.J. Elsey, J.R.S. Greenhalgh, B.F. Schutz, D. Nicholson, J.R. Shuttleworth, J. Ehlers, P. Kafka, G. Schäfer, H. Braun, and V. Kose, Lecture Notes in Physics 410 (1992) 184.

[9] C. Zener, Elasticity and Anelasticity of Metals (Univ. of Chicago, Chicago, 1948).

[10] P.R. Saulson, Phys. Rev. D 42 (1990) 2437.

[11] Catalog of Goodfellow Corp.

[12] N.G. McCrum, B.E. Read, and G. Williams, Anelastic and Dielectric Effects in Polymeric Solids (John Wiley & Sons, London, 1967).

[13] C.C. Speake, Proc. R. Soc. London A 414 (1987) 333.

[14] V.B. Braginsky, V.P. Mitrofanov, and O.A. Okhrimenko, JETP Lett. 55 (1992) 432.

[15] D.B. Fraser, J. Appl. Phys. 41 (1970) 6.

[16] LIGO Team, "Installation of New Test Masses in LIGO 40 Meter Interferometer", LIGO Technical Report TR94-7, November 30, 1994.

[17] P.R. Saulson, and A. Abramovici, "Test Mass Creep Measurements as a Probe of Low Frequency Internal Friction", talk at First International Workshop on Thermal Noise in Laser Interferometer Gravitational-Wave Detectors, Caltech, January 4-5, 1994.

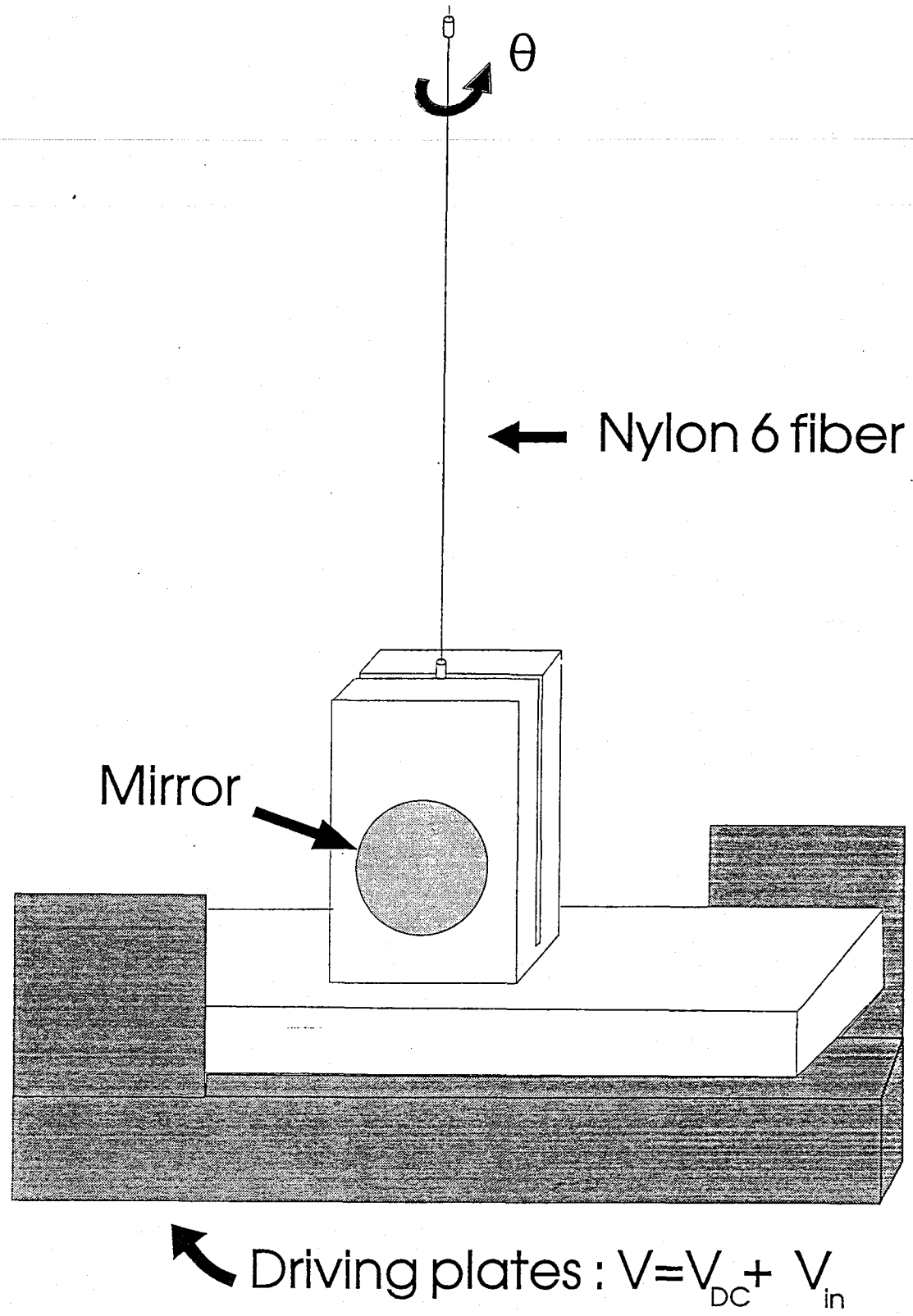
θ
Nylon 6 fiber
Mirror
Driving plates : V=V_DC+ V_in

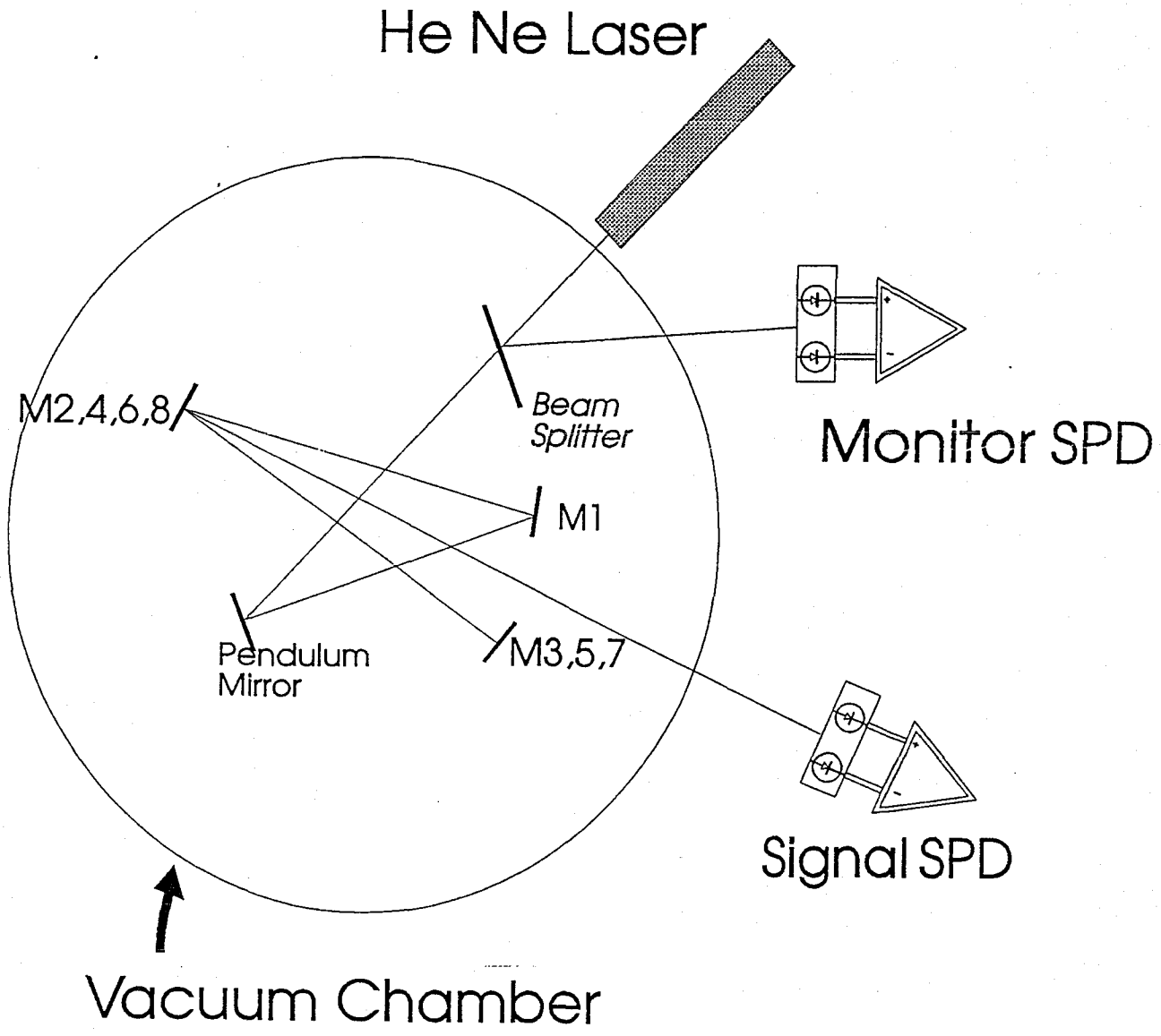
He Ne Laser
Monitor SPD
Beam
Splitter
M2,4,6,8
M1
Pendulum
Mirror
M3,5,7
Signal SPD
Vacuum Chamber

Figure 3a: Frequency response (amplitude)

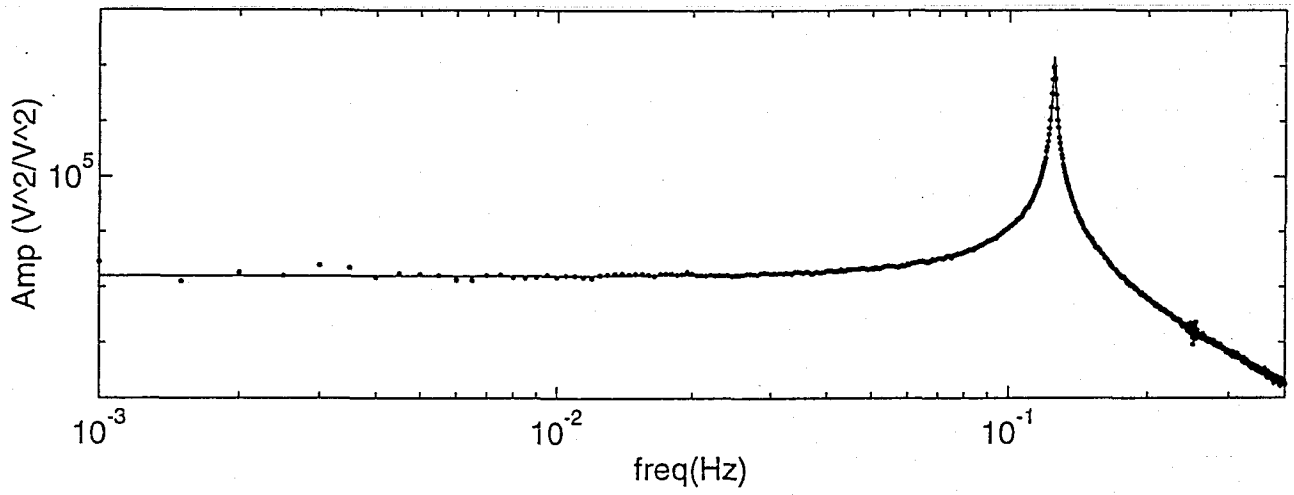

Figure 3b: frequency response (loss angle)

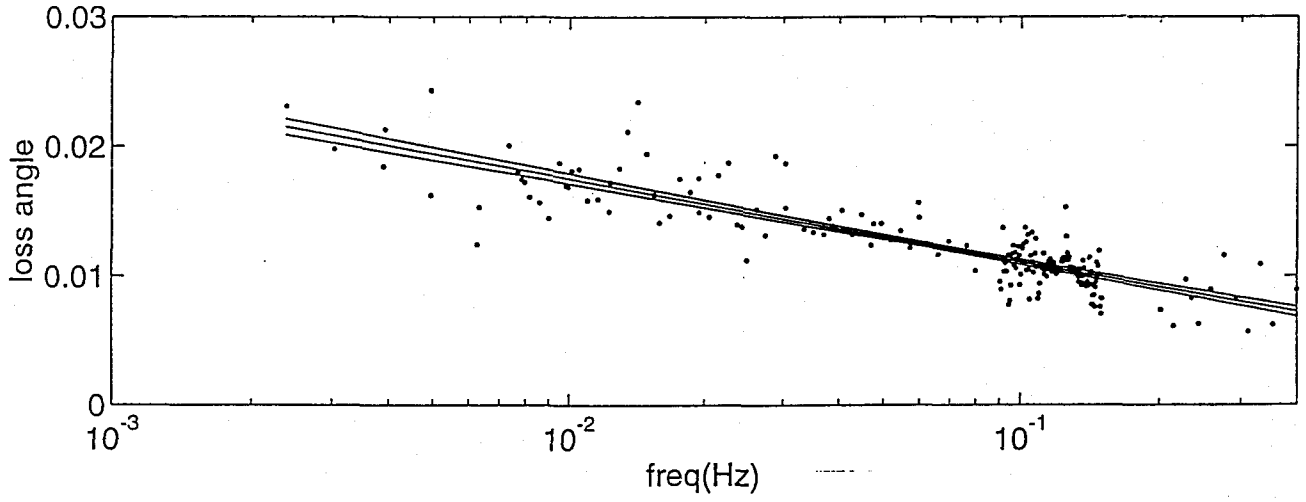

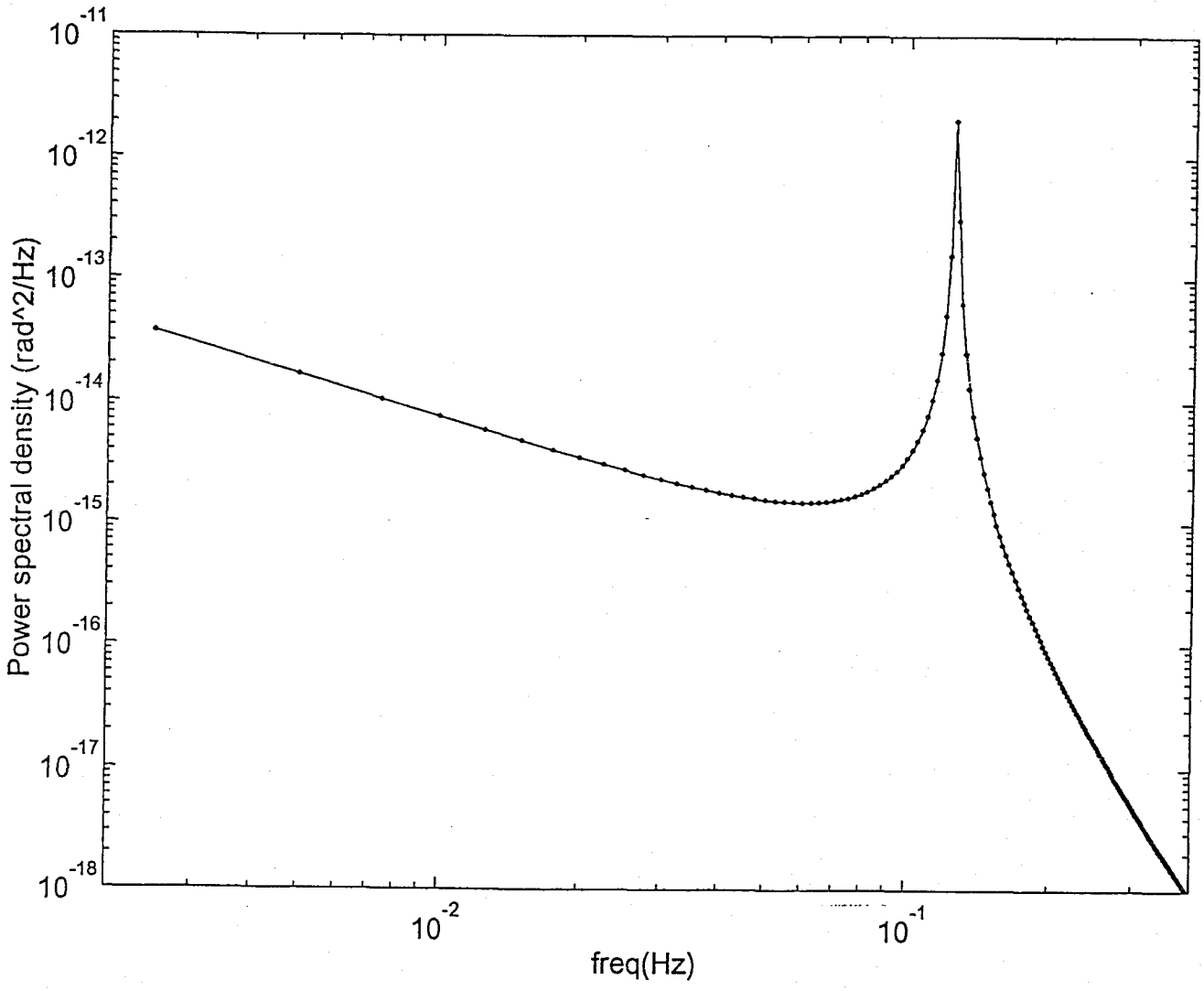
Power spectral density (rad^2/Hz)
10^-11
10^-12
10^-13
10^-14
10^-15
10^-16
10^-17
10^-18
10^-2
10^-1
freq(Hz)

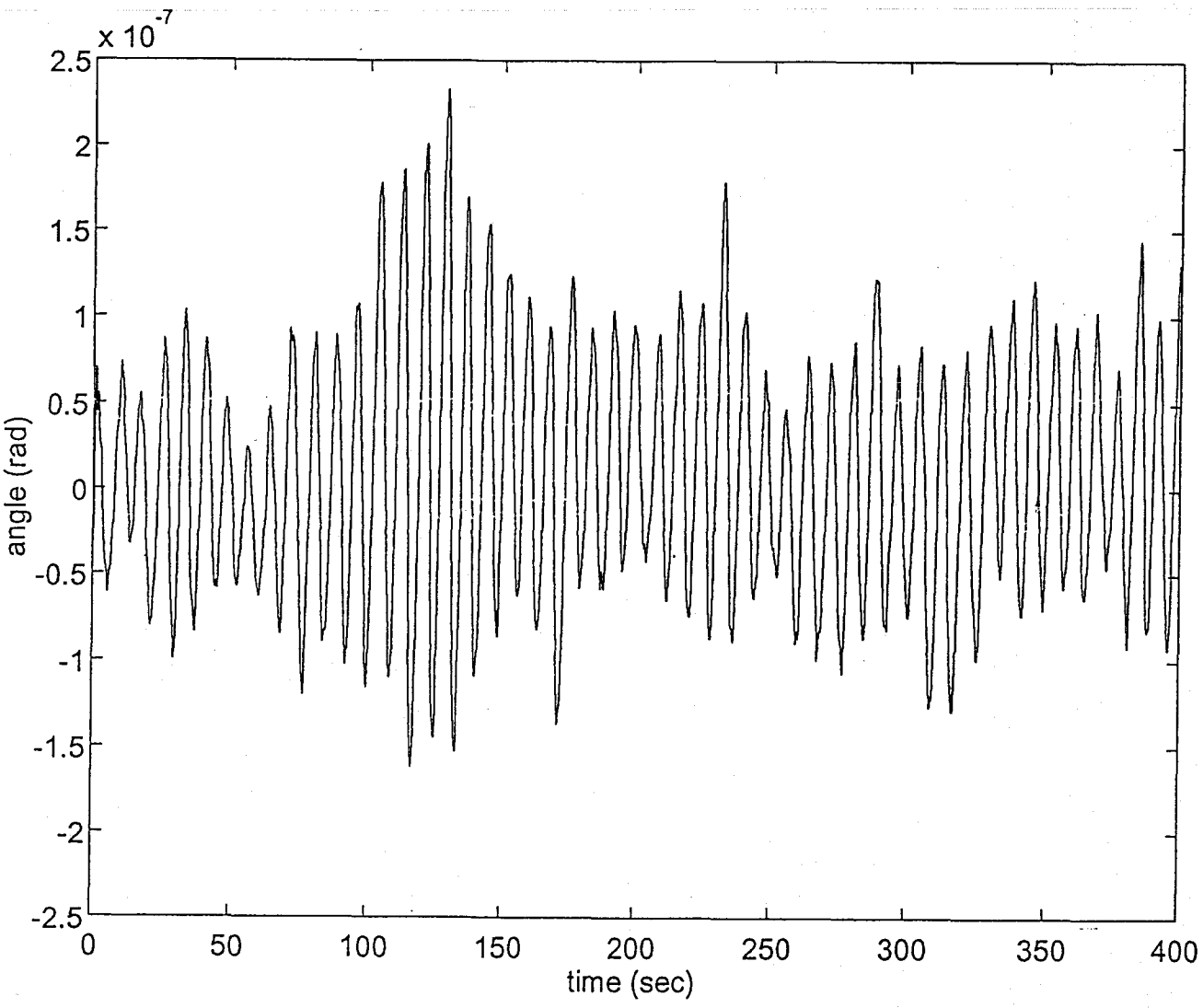
x 10^-7
2.5
2
1.5
1
0.5
0
-0.5
-1
-1.5
-2
-2.5
angle (rad)
0
50
100
150
200
250
300
350
400
time (sec)

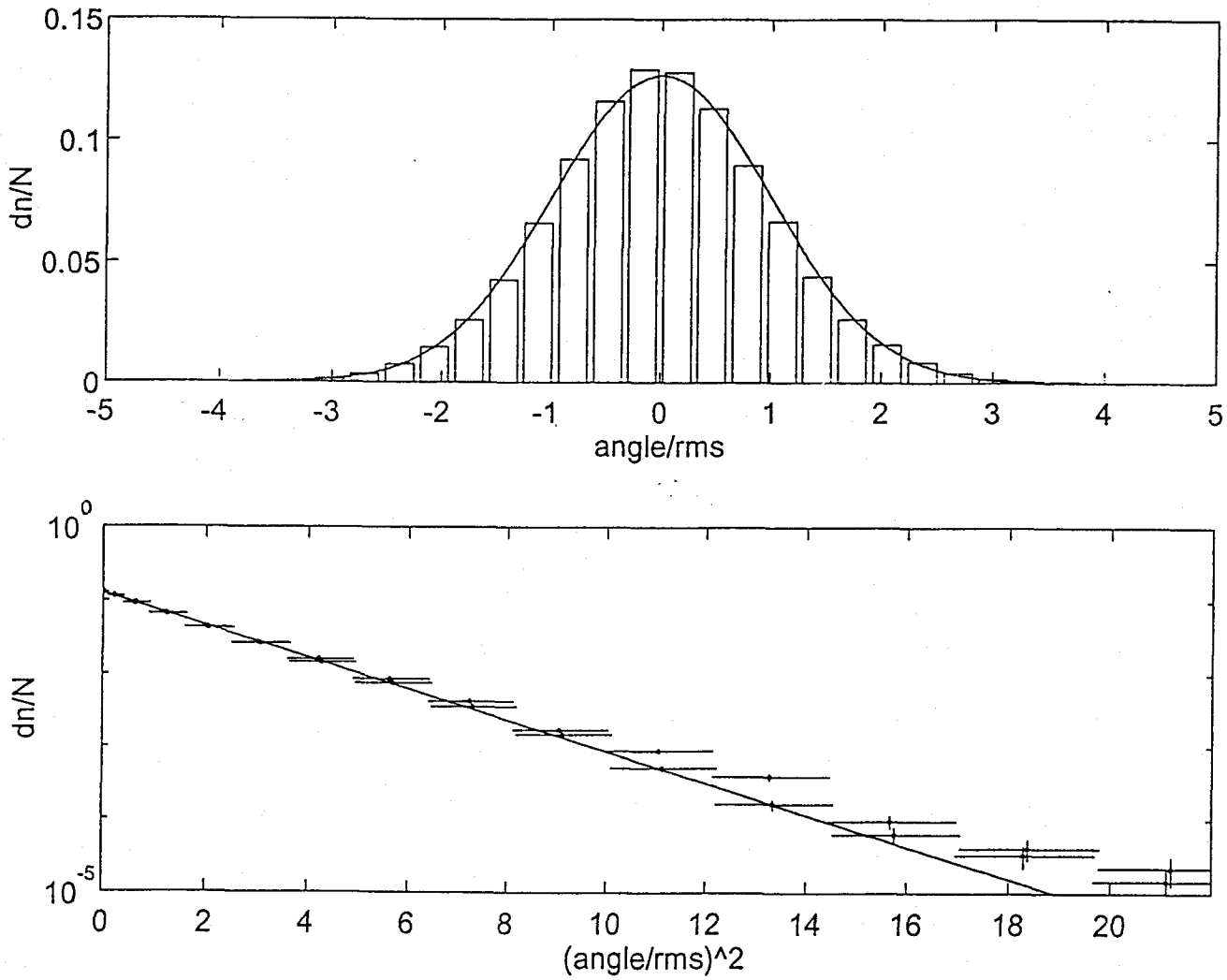
0.15
0.1
0.05
0
dn/N
-5
-4
-3
-2
-1
0
1
2
3
4
5
angle/rms
10^0
10^-5
dn/N
0
2
4
6
8
10
12
14
16
18
20
(angle/rms)^2

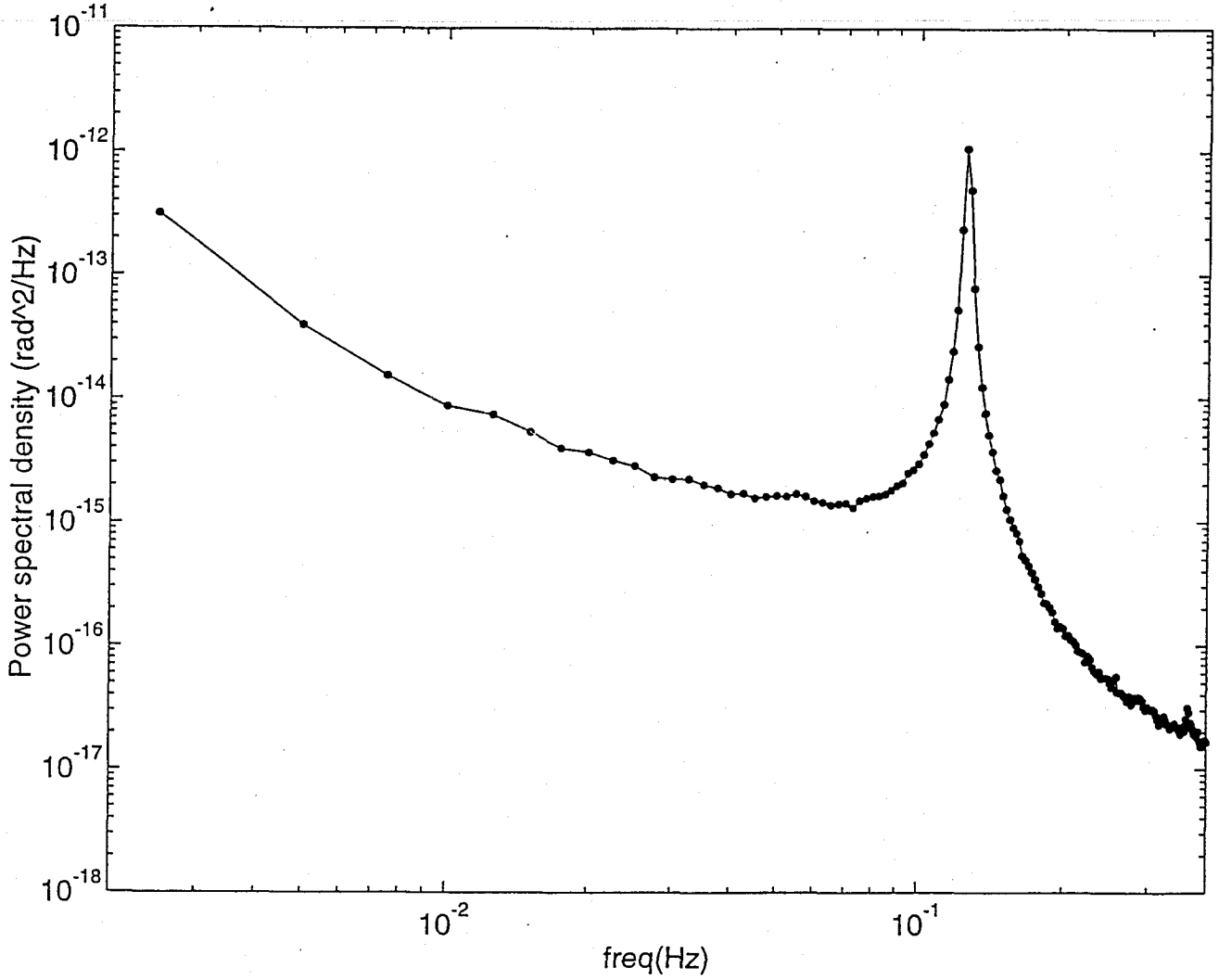
Power spectral density (rad^2/Hz)
10^-11
10^-12
10^-13
10^-14
10^-15
10^-16
10^-17
10^-18
10^-2
10^-1
freq(Hz)

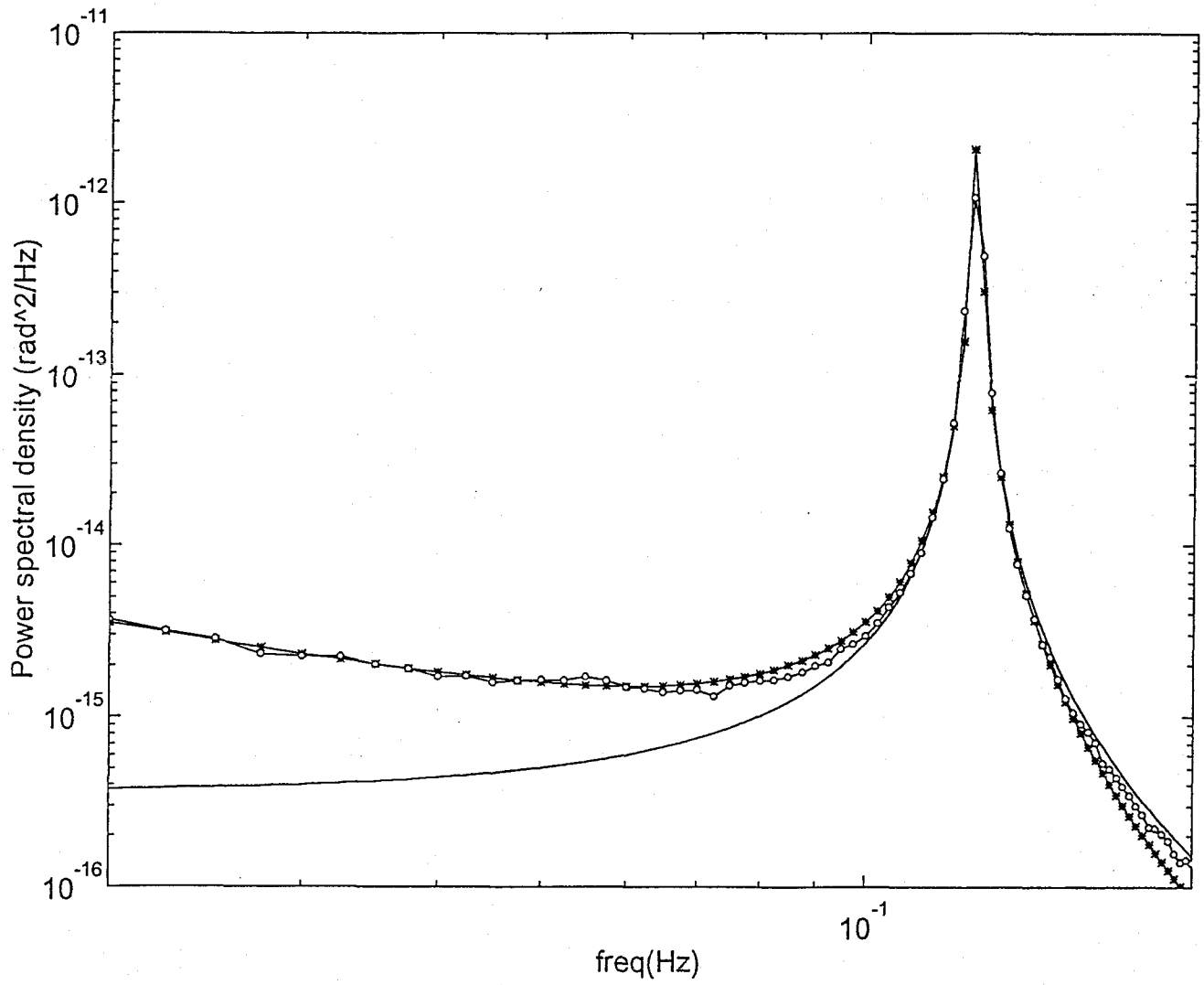
Power spectral density (rad^2/Hz)
10^-11
10^-12
10^-13
10^-14
10^-15
10^-16
10^-1
freq(Hz)

Figure Captions

Figure 1: The torsion pendulum and the driving plates.

Figure 2: Optical lever schematic. The total optical path, from the pendulum mirror to the measuring photocell is 155 cm (folded in the vacuum chamber by mirrors M1-8).

Figure 3: Frequency response measurement: magnitude and loss angle (eqns. 2.5 and 2.6). The solid line in Fig. 3a is a fit to the amplitude according to eqn. 2.5, and the solid lines in Fig. 3b are a linear fit (eqn. 4.1) and its 95% confidence level interval.

Figure 4: Thermal noise spectrum predicted from the frequency response measurement, using the fluctuation-dissipation theorem (eqn. 2.4).

Figure 5: Portion of a typical time record of angular Brownian motion of the torsion pendulum.

Figure 6: Histogram of the amplitude of 30 hours of time records, sampled at a 5.12 Hz frequency (273,000 points). The lower figure shows the count fraction per bin, with positive and negative angles folded into $(\theta/\theta_{rms})^2$. The error bars are the statistical error $(1/\sqrt{n})$ and the bin width chosen for the histogram.

Figure 7: Power spectral density of Brownian motion, averaged over 30 hrs

of time records. The point size represents the measurement statistical errors.

Figure 8: Comparison between the predicted Brownian motion power spectrum in Fig. 4 (asterisks) and the measured power spectrum in Fig. 7 (filled circles). There are no adjustable parameters in the comparison. The dotted line would be the prediction of the fluctuation-dissipation theorem using a viscous friction model with the same Q at resonance.